

Adaptive Type-2 Fuzzy Sliding Mode Control for Grid-Connected Wind Turbine Generator Using Very Sparse Matrix Converter

Muldi Yuhendri^{***‡}, M. Ashari^{*}, M. H. Purnomo^{*}

^{*}Department of Electrical Engineering, Institut Teknologi Sepuluh Nopember, Surabaya

^{**}Department of Electrical Engineering, Universitas Negeri Padang, Padang

(muldiyuhendri@gmail.com, ashari@ee.its.ac.id, hery@ee.its.ac.id)

[‡]Corresponding Author; Muldi Yuhendri, Department of Electrical Engineering, Universitas Negeri Padang, Padang

muldiyuhendri@gmail.com

Received: 16.03.2015-Accepted:29.04.2015

Abstract-The strategy to improve both efficiency and power quality of grid-connected wind turbine generator systems (WTGs) are presented. WTGs efficiency is improved by developing a variable speed control to obtain maximum power at all wind speeds. Variable speed control based on Adaptive Type-2 Fuzzy Sliding Mode Control (AFSMOC) is proposed by employing Very Sparse Matrix Converter (VSMC). Type-2 fuzzy system is used to improve the robustness of sliding mode control. VSMC can provide low harmonics in line current, so the power quality problems can be minimized. The simulation results shows that the AFSMOC can regulate the generator speed at optimum Tip Speed Ratio (TSR) with maximum error 2.5 rpm, so that the maximum power can be obtained at all wind speeds. VSMC also provide good performance with Total Harmonic Distortion (THD) of voltage 0.35% and THD of current 6,82%.

Keywords-Wind turbine generator; very sparse matrix converter; adaptive type-2 fuzzy sliding mode control; variable speed control.

1. Introduction

The Wind turbine generator system (WTGs) is one of the ways to deal with the growing electric energy demands in Indonesia. WTGs widely developed with variable speed operation because it can increase the efficiency with maximum output power and widen the operating range at all wind speeds [1,2]. Variable speed WTGs many uses Permanent Magnet Synchronous Generator (PMSG) due many advantages such as self excitation, easy to control, smaller in size, and has a high efficiency with the absence of rotor losses [3,4].

Generally, variable speed control of WTGs using power converter. Various types of converters have been applied to WTGs. Converter types widely used for PMSG-wind turbine are back to back converter, dioda rectifier-inverter and matrix converter [5,6]. Multilevel inverter also been applied

to improve the voltage quality of WTGs [7]. Matrix converter is the best alternative to the grid-connected WTGs because higher efficiency with increased power density, not dc-link storage and low THD in line current [8,9]. One of the disadvantages of conventional matrix converter is using a lot of switches, so it becomes expensive. To resolve this problem has developed several models of sparse matrix converter [10,11], and one of the models that have been used for WTGs is VSMC [12].

In this paper, variable speed control of grid-connected PMSG-wind turbine is proposed by using VSMC. The PMSG speed is controlled at optimum point of TSR to obtain maximum power at all wind speeds. The PMSG speed control many developed by Field Oriented Control (FOC). This method is applied with decoupled control of torque and flux through the stator current in direct-quadrature axis (i_d, i_q). Several control strategies have been implemented for

FOC, One is Sliding Mode Control (SMC) [13,14]. SMC has received much attention due robust to disturbances [13].

To improve the robustness, SMC can be developed with adaptive gain. Wavelet neural network and extended state observer for adaptive gain of SMC has been discussed in [13,14]. In this paper, adaptive gain of SMC is proposed by using type-2 fuzzy system (T2FS). It is more attractive to handle the uncertainty of membership function parameters, so that the adaptive gain becomes more valid to improve the SMC performances [15,16]. It will improve the performance of variable speed control of grid-connected PMSG-wind turbine.

2. Wind Turbine Generator System Modeling

The proposed variable speed control of grid-connected PMSG-wind turbine is shown in Fig. 1. The proposed system consists of horizontal wind turbine, PMSG connected to the grid through VSMC, resistive load and speed controller. Small LC filter is placed on the grid side to improve the quality of both the voltage and current. The speed controller is developed by using FOC method based on constant torque angle control. In this method, decoupled control of torque and flux is applied by adjust the stator current in direct-quadrature axis (i_d, i_q). AFSMOC is applied to obtain the reference of q -axis stator current i_q^* based on speed error, while the reference of d -axis stator current i_d^* is kept zero. To obtain the reference voltage (v_d^* and v_q^*) for modulate a VSMC, both i_d^* and i_q^* are regulated by SMC.

2.1. Permanent Magnet Synchronous Generator Modeling

The dynamic model of Permanent Magnet Synchronous Generator (PMSG) for variable speed control in FOC method are projected in dq -axis of rotating synchronous reference frame. In this scheme, the dq -axis stator current (i_d and i_q) can be written as :

$$\frac{d}{dt} \begin{bmatrix} i_d \\ i_q \end{bmatrix} = \begin{bmatrix} -\frac{R_s}{L_d} & \omega_e \\ -\omega_e & -\frac{R_s}{L_q} \end{bmatrix} \begin{bmatrix} i_d \\ i_q \end{bmatrix} + \begin{bmatrix} \frac{v_d}{L_d} \\ \frac{v_q}{L_q} - \omega_e \frac{\psi_m}{L_q} \end{bmatrix} \quad (1)$$

where R_s , ω_e , n_p and ψ_m are the stator resistance, the electrical speed, the number of pole pairs and the flux of permanent magnet, respectively. L_d , L_q , and v_d, v_q are the stator inductances and the stator voltages in dq -axis, respectively.

PMSG speed control using AFSMOC is applied by regulating the electromagnetic torque T_e through q -axis stator current i_q control based on the mechanical dynamic of PMSG, as in Eq. (2). The relationship between T_e and i_q is expressed in Eq. (3).

$$\frac{d}{dt} \omega_m = \frac{T_m - T_e - B\omega_m}{J} \quad (2)$$

$$T_e = -1.5 n_p \psi_m i_q \quad (3)$$

where ω_m , T_e , T_m , B and J are the mechanical speed, the electromagnetic torque, the mechanical torque, the friction coefficient and the inertia moment, respectively. The output power of PMSG P_o is :

$$P_o = \frac{3}{2} (v_d i_d + v_q i_q) \quad (4)$$

2.2. Very Sparse Matrix Converter Modeling

Very Sparse Matrix Converter (VSMC) is one type of indirect matrix converter which uses 12 active switches. The structure of VSMC can be seen in Fig. 1.

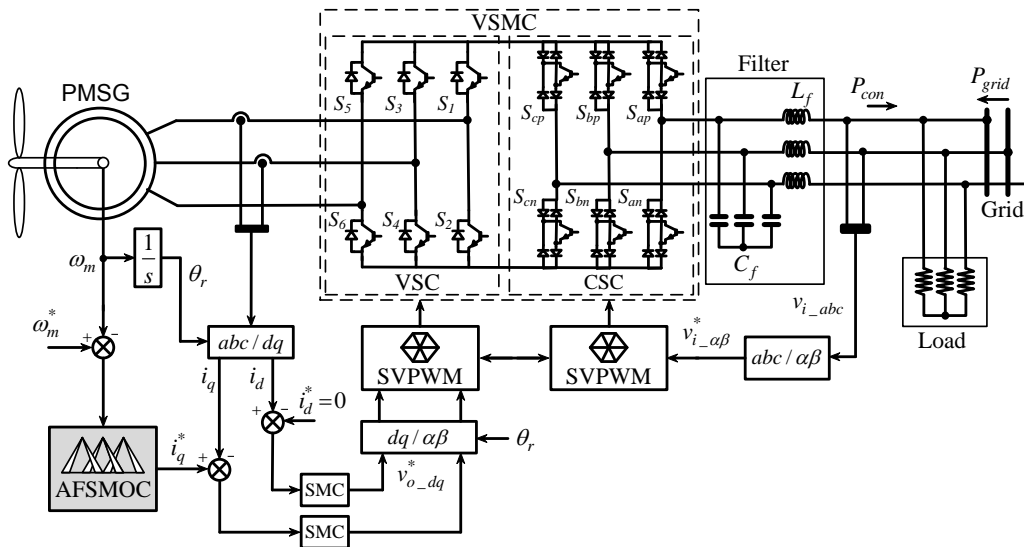


Fig. 1. The structure of variable speed control the PMSG wind turbine

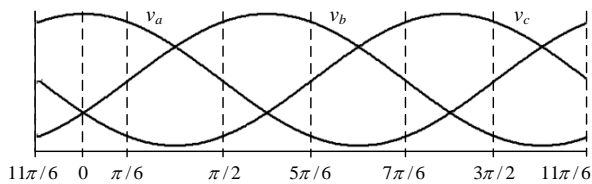
This type less expensive than conventional indirect matrix converter which uses 18 active switches. The main difference between direct matrix converter with indirect matrix converter is in the switches structure. The direct matrix converter switches arranged in a matrix form, whereas the indirect matrix converter switches is organized into two groups converter as a back-to-back converter, so that the modulation strategies of indirect matrix converter easier than direct matrix converter.

VSMC consists of the current source converters (CSC) and the voltage source converters (VSC) as shown in Fig.1. The advantages of VSMC is not using the DC-link energy storage that require large size capacitor. As a replacement, small LC filter is employed to reduce the input harmonics. In this paper, VSMC is modulated by using Space vector modulation.

The modulation strategy of the CSC switches is to generate the maximum dc-link voltage and keep unity input power factor. The switching states of CSC are determined based on the space vector of the input voltages that are divided into 6 sectors, as shown in Fig. 2a. The duty cycle of the CSC switches in $\alpha\beta$ for sector 1 are :

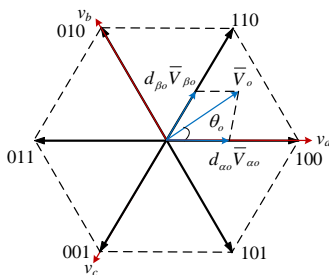
$$\begin{aligned} d_{\alpha i} &= -(i_b/i_a) = -(v_b/v_a) \\ d_{\beta i} &= -(i_c/i_a) = -(v_c/v_a) \\ d_{\alpha i} + d_{\beta i} &= 1 \end{aligned} \tag{5}$$

The duty cycle of CSC switches for each sector can be calculated based on Eq. (5) and the space vector of the input voltage in Fig. 2a.



Sector	1	2	3	4	5	6
$d_{\alpha i}, d_{\beta i}$	S_{bn}, S_{cn}	S_{ap}, S_{bp}	S_{cn}, S_{an}	S_{bp}, S_{cp}	S_{an}, S_{bn}	S_{cp}, S_{ap}
$d_{\alpha i} + d_{\beta i}$	S_{ap}	S_{cn}	S_{bp}	S_{an}	S_{cp}	S_{bn}

(a)



(b)

Fig. 2. The switching state of VSMC for each sector, (a) CSC stage, (b) VSC stage

The VSC switches are modulated based on space vector of the output voltages, that are separated by 6 sectors as shown in Fig. 2b. The duty cycle of the VSC switches are :

$$\begin{aligned} d_{\alpha o} &= m_o \sin\left(\frac{\pi}{3} - \theta_o\right) \\ d_{\beta o} &= m_o \sin\left(\frac{\pi}{3}\right) \\ d_{0o} &= 1 - d_{\alpha o} - d_{\beta o} \end{aligned} \tag{6}$$

where $m_o = 4\bar{V}_o/3\bar{V}_i$ is modulation index. θ_o , \bar{V}_o and \bar{V}_i are the output voltage angle, the output voltage amplitude and the input voltage amplitude, respectively.

To balance the input currents and the output voltages, the CSC switches must be coordinated with the VSC switches. Note that the states change of the CSC switches always occurs during free-wheeling condition of the VSC switches. Fig. 3 shows the coordination between the CSC switches with the VSC switches for sector 1.

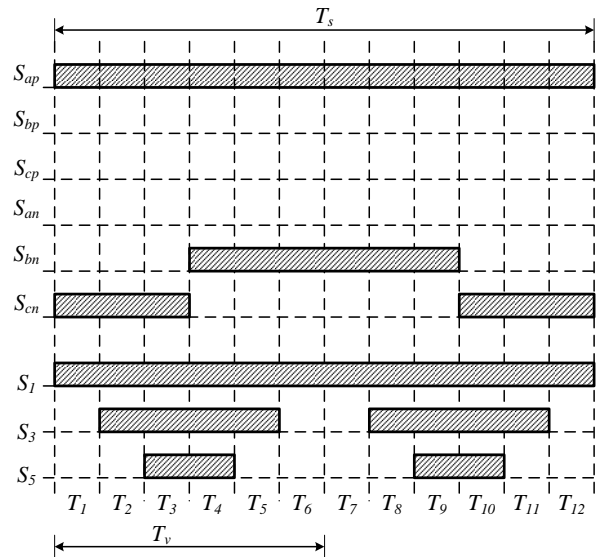


Fig. 3. The coordination between CSC with VSC for sector 1

Figure 3 shows that each switching period of the CSC switches T_s , there are two switching period of the VSC switches T_v . One switching period of CSC switches divided into 12 switching times, as in Eq. (7). The modulation pulses are achieved by compare the switching time with linear carrier pulse.

$$\begin{aligned} T_1 = T_{12} &= 0.5 d_{\beta i} d_{\alpha o}, & T_4 = T_9 &= 0.5 d_{\alpha i} d_{0o} \\ T_2 = T_{11} &= 0.5 d_{\beta i} d_{\beta o}, & T_5 = T_8 &= 0.5 d_{\alpha i} d_{\beta o} \\ T_3 = T_{10} &= 0.5 d_{\beta i} d_{0o}, & T_6 = T_7 &= 0.5 d_{\alpha i} d_{0o} \\ T_s &= T_1 + T_2 + \dots + T_{12} = 1 \end{aligned} \tag{7}$$

2.2.2.3. Wind Turbine Modeling

Based on the aerodynamic characteristics, the mechanical power available from a wind turbine P_m to drive PMSG can be written as :

$$P_m = 0.5 \pi R^2 C_p (\lambda, \beta) \rho v_w^3 \tag{8}$$

where ρ is the air density. R is the blade radius, v_w is the wind speed and C_p is power coefficient of turbine, which is a function of the tip speed ratio (TSR) λ and the pitch angle β . TSR depends on the rotor speed, which can be written as :

$$\lambda = \frac{\omega_m R}{v_w} \tag{9}$$

Based on Eq. (8) and (9), the mechanical power P_m of wind turbine also depends on the rotor speed ω_m . Figure 4 shows the mechanical power curve versus rotor speed. For each wind speed, there exists a maximum power point. Wind turbine can achieve the maximum power point P_{mmax} when operating at maximum power coefficient C_{pmax} and optimum TSR λ_{opt} [17], which is written as :

$$P_{m_max} = 0.5 \pi R^2 \rho C_{p_max} (\lambda_{opt}, \beta) v_w^3 \tag{10}$$

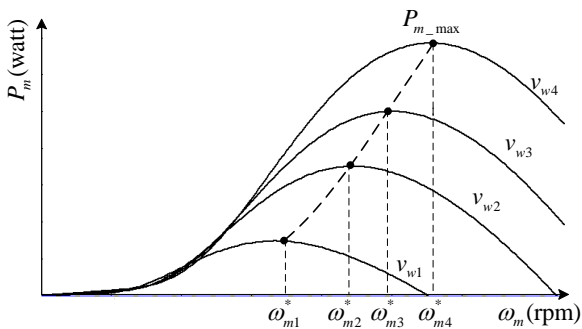


Fig. 4. The mechanical power curve of wind turbine

Variation of wind speed generates maximum power point located at different rotor speeds, as shown in Fig. 4. The reference speed ω_m^* for maximum power is given by :

$$\omega_m^* = v_w \frac{\lambda_{opt}}{R} \tag{11}$$

To obtain maximum power at all wind speed, variable speed control is required to maintain the wind turbine operation at optimum TSR. In this paper, variable speed control of PMSG wind turbine is proposed using AFSMOC.

3. PMSG Speed Control Based on AFSMOC

Variable speed control of PMSG is proposed by using Adaptive Type-2 Fuzzy Sliding Mode Control (AFSMOC) based on Field oriented control. In this method, the PMSG speed is controlled by regulating the electromagnetic torque through q -axis stator current control, while the d -axis stator current is kept zero. AFSMOC is applied to regulate the reference of q -axis stator current i_q^* based on speed error e_ω .

Figure 5 shows the structure of AFSMOC for PMSG speed control.

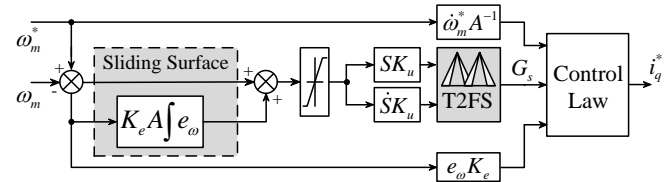


Fig. 5. The structure of AFSMOC.

The structure of AFSMOC consists of the sliding surface stage, the adaptive gain stage and the control law stage. T2FS is applied to obtain the adaptive gain G_s , so that the robustness of speed controller can be improved.

PMSG speed control using AFSMOC is developed from mechanical dynamic of PMSG in Eq. (2). The mechanical dynamics of PMSG with parameter variations due system disturbances can be formulated from Eq. (2) and Eq. (3) as follows :

$$\frac{d}{dt} \omega_m = (1.5 n_p \psi_m i_q^* / J) + K_t \tag{12}$$

$$K_t = (T_m - 1.5 n_p \psi_m (i_q^* - i_q) - B \omega_m) / J \tag{13}$$

where K_t is the lumped dirturbances of system. The control law of AFSMOC to obtain i_q^* is given by :

$$i_q^* = K_e e_\omega + G_s \text{sat} \left(\frac{S}{\phi} \right) + \left(\frac{d}{dt} \omega_m^* A^{-1} \right) \tag{14}$$

with

$$e_\omega = \omega_m^* - \omega_m \text{ and } A = 1.5 \frac{n_p \psi_m}{J} \tag{15}$$

where G_s is adaptive gain obtained from T2FS, ω_m is the measured speed, ω_m^* is the reference speed obtained from Eq. (11), K_e is the speed error gain and S is the sliding surface which is given by :

$$S = e_\omega + A K_e \int_0^t e_\omega dt \tag{16}$$

with saturation function of sliding surface :

$$\text{sat} \left(\frac{S}{\phi} \right) = \begin{cases} 1 & S > \phi \\ \frac{S}{\phi} & -\phi < S < \phi \\ -1 & S < -\phi \end{cases} \tag{17}$$

Where ϕ is a constant. The AFSMOC performances are determined by K_e and G_s . It is verified using Lyapunov function. Assume that the lumped dirturbances of system in Eq. (13) satisfies $0 \leq |K_t| < h$. Using Eq. (14), the speed converges to zero if $G_s > A^{-1}h$. If the Lyapunov function is

defined as $V = 0.5 S^2$, the derivative of the Lyapunov function can be formulated by using Eq. (14) as follow:

$$\begin{aligned} \frac{d}{dt} V &= \frac{d}{dt} S S = S \left(\frac{d}{dt} e_\omega + A K_e e_\omega \right) \\ &= -A S \left(i_q^* + A^{-1} K_t - K_e e_\omega - A^{-1} \frac{d}{dt} \omega_m^* \right) \\ &= -A \left(G_s |S| + A^{-1} S K_t \right) \\ &\leq -A |S| \left(G_s - A^{-1} h \right) < 0 \quad (S \neq 0) \end{aligned} \quad (18)$$

The theorem is proved if Eq. (14) makes Eq. (16) converge to zero.

3.1. Type-2 Fuzzy System

Type-2 Fuzzy System (T2FS) is used to obtain the adaptive gain of AFSMOC (G_s) with inputs are the sliding surface $s = S K_u$ and ~~the its derivatives of sliding surface~~ $d_s = \dot{S} K_u$ where K_u is the T2FS input gain.

The T2FS structure consists of fuzzifier, rule base, fuzzy inference engine, type-reducer and defuzzifier [15,16]. In fuzzifier, the input values are mapping into the membership function, which is presented by upper membership function and lower membership function. The interval between these two function represent the footprint of uncertainty (FOU), which is used to characterize a type-2 fuzzy set. Triangular membership function with uncertain width is used in this paper, as shown in Fig. 6.

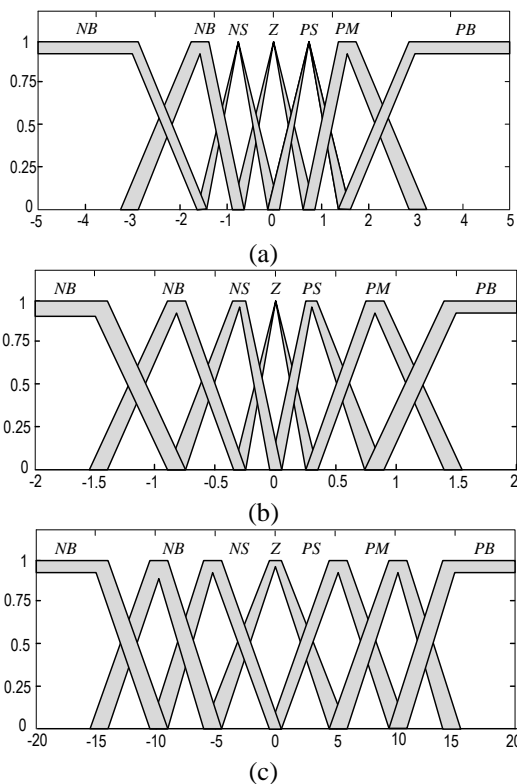


Fig. 6. Membership function of T2FS. (a) the input s , (b) the input d_s , (c) the output G_s

The i -th T2FS rules can be written as :

$$R^i = \text{IF } s \text{ is } X_s^i \text{ and } d_s \text{ is } X_{ds}^i \text{ THEN } G_s \text{ is } Y^i \quad (19)$$

with

$$X_s, X_{ds}, G_s \subseteq [NB, NM, NS, Z, PS, PM, PB] \quad (20)$$

where X_s and X_{ds} are fuzzy set of the input, G_s is fuzzy set of the output. N and P denote the negative and positive of the membership functions. $i = 1, \dots, n$. The rule base of T2FS is listed in Table 1.

Table 1. Rule base of T2FS

$s \backslash d_s$	NB	NM	NS	Z	PS	PM	PB
PB	Z	PS	PS	PM	PM	PB	PB
PM	NS	Z	PS	PS	PM	PM	PB
PS	NS	NS	Z	PS	PS	PM	PM
Z	NM	NS	NS	Z	PS	PS	PM
PS	NM	NM	NS	NS	Z	PS	PS
PM	NB	NM	NM	NS	NS	Z	PS
PB	NB	NB	NM	NM	NS	NS	Z

The firing strength of the i -th rule can be expressed as :

$$F^i = \left[\underline{f}^i \quad \bar{f}^i \right] \quad (21)$$

$$\underline{f}^i = \underline{\mu}_{X_s}(s) \times \underline{\mu}_{X_{ds}}(d_s) \text{ and } \bar{f}^i = \bar{\mu}_{X_s}(s) \times \bar{\mu}_{X_{ds}}(d_s) \quad (22)$$

where $\underline{\mu}$ and $\bar{\mu}$ denote the lower membership function and the upper membership function, respectively. Using the center of set (COS) type-reduction, the output fuzzy T2FS can be written as :

$$Y_{COS} = [y_l, y_r] \quad (23)$$

where Y_{COS} is an interval type-1 set. y_l and y_r are the left end point or the minimum value of y and the right end point or the maximum value of y , respectively. y_l and y_r can be computed using the Karnik-Mendel algorithm as follows :

$$y_l = \frac{\sum_{i=1}^L \bar{f}^i w_l^i + \sum_{i=L+1}^M \underline{f}^i w_l^i}{\sum_{i=1}^L \bar{f}^i + \sum_{i=L+1}^M \underline{f}^i} \quad (24)$$

$$y_r = \frac{\sum_{i=1}^R \underline{f}^i w_r^i + \sum_{i=R+1}^M \bar{f}^i w_r^i}{\sum_{i=1}^R \underline{f}^i + \sum_{i=R+1}^M \bar{f}^i} \quad (25)$$

where w_l, w_r are the consequent centroid set with interval ($i = 1, \dots, M$), while M is the total number of rules in the rule base of a T2FS. The adaptive gain of AFSMOC G_s is obtained from the defuzzified crisp output as follows :

$$G_s = y = \frac{y_l + y_r}{2} \quad (26)$$

4. Simulation Results

The proposed grid-connected WTGs in Fig. 1 is verified by using matlab simulink. The proposed WTGs using PMSG 3HP driven by horizontal wind turbine with blade radius 2 m. WTGs are connected to a grid 220V, 50 Hz, with resistive load 1.5 kW. The Simulation parameters listed in appendix. The proposed system are simulated with variable wind speed, as shown in Fig. 7.

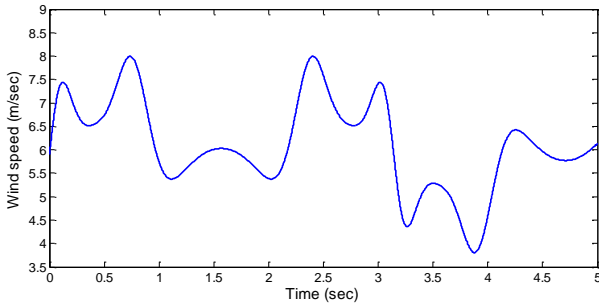


Fig. 7. Wind speed

The performances of AFSMOC to regulate PMSG speed is shown in Fig. 8. The rotor speed can be regulated at reference speed for all wind speeds, as shown in Fig. 8a. This shows the good performance of AFSMOC to control the rotor speed at optimum TSR, so that the maximum power can be obtained. Figure 8b shows the TSR graph. Wind turbine has the optimum TSR 8.09. Figure 8b shows that the rotor speed can achieve the maximum point at 0.23 seconds.

When the rotor speed is around the optimum point, TSR always under optimum TSR. This is due to the ever-changing wind speed. The reference speed for maximum power point is always changing according to the change of wind speed and always leading from the measured speed. This causes the speed error always be above zero with maximum error 2.3 rpm, as shown in Fig. 8.c. However, the rotor speed remains around the maximum point at all wind speed. This is indicated by the low error of TSR. The maximum error of TSR is 0.03, as shown in Fig. 8b. So it can be concluded that the generator can reach the point of maximum power at all wind speeds, despite the extreme changes of wind speed. Figure 7 shows that the wind speed decrease drastically at a time 0.8 seconds and 3 seconds. Vice versa, an increase drastically at a time 2 seconds and 3.8 seconds. The robustness of AFSMOC in controlling the rotor speed has made the rotor speed remains at the maximum power point, despite drastic changes in wind speed.

The robustness of AFSMOC looks from the electromagnetic torque response with low distortion in Fig. 8d, as well as the q-axis stator current in Fig.8e. AFSMOC still able to control the rotor speed at the maximum power point with low distortion of the electro magnetic torque when there is an extreme change of wind speed at time 3 second. This shows that the adaptive gain from T2FS has worked well to improve the robustness of SMC to handle the uncertainty of parameters due disturbances.

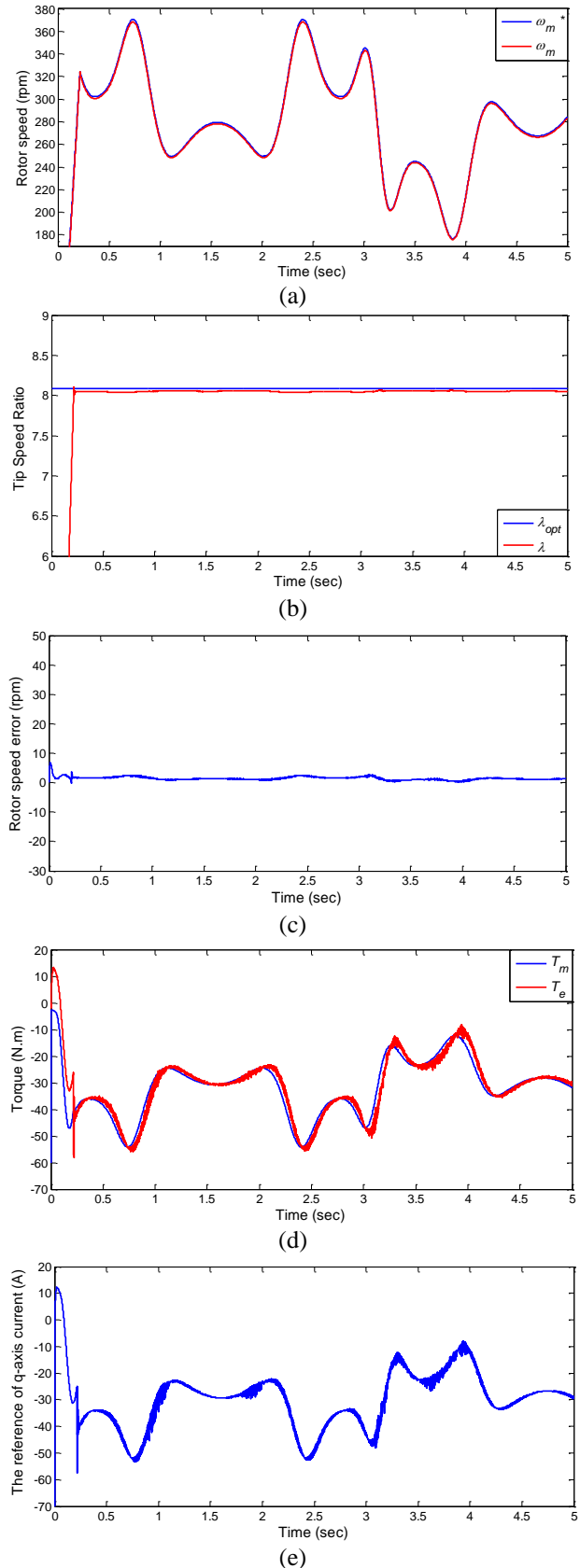


Fig. 8. The performances of AFSMOC. (a) Rotor speed, (b) TSR, (c) rotor speed error, (d) elektro magnetic torque, (e) q-axis stator current

The AFSMOC performances to regulate the rotor speed at maximum power point also can be seen from power coefficient in Fig. 9a, that are always at the maximum point

0.5312 at all wind speeds. Figure 9b shows the power flow from WTGs P_{con} to resistive load. Power flow of WTGs decrease the power supply from the grid P_{grid} to load. The highest power flows from the generator to the load occurs when the wind speed of 8 m/s at time 3 seconds. This indicates that the VSMC are functioning properly.

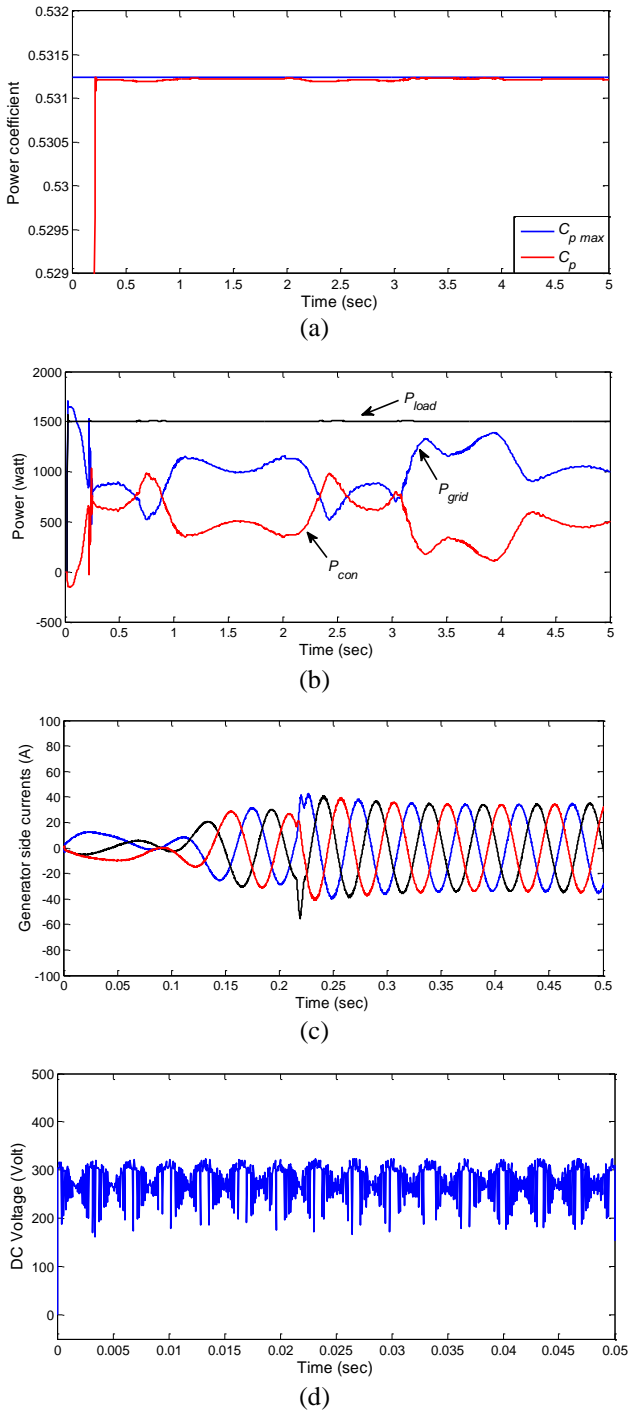


Fig. 9. (a) power coefficient (b) power (c) generator currents (d) DC-Link voltages results.

The generator side currents in Fig. 9c shows that a VSMC has functioned well as a frequency converter for variable speed control of WTGs. The generator type used is

sinusoidal PMSG, so that also produces a sinusoidal current in generator side, as shown in Fig. 9c.

Figure 9d shows that the modulation strategies of CSC stage has produced maximum DC-link voltage so that the maximum voltage transfer ratio can be obtained. Due to the zero-voltage vector cancellation in CSC modulation, the DC-link voltage does not consist of the zero voltage level, as shown in Fig. 9d.

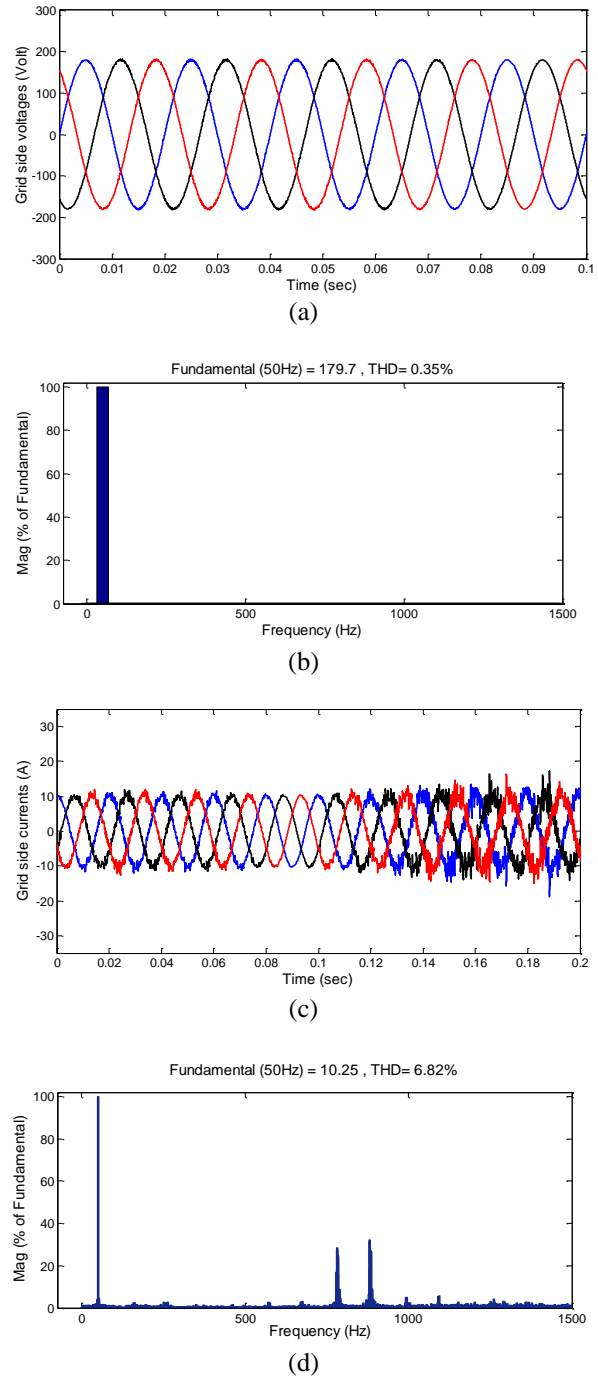


Fig. 10.(a) grid side voltages (b) THD of voltages, (c) grid side currents, (d) THD of currents

Small LC filter at grid side can reduce harmonics due switching frequency of converter. Both sinusoidal voltage and sinusoidal current at a gridside can be achieved, as shown in Fig. 10a and Fig. 10c. Low harmonic of grid side voltage can be seen in Fig. 10b with THD 0.35%, while the THD of current 6.82%, as shown in Fig. 10d. This indicates that the VSMC has advantages for grid-connected WTGs.

5. Conclusion

Variable speed control of grid-connected PMSG wind turbine using VSMC based on has been discussed. The PMSG speed is controlled by AFSMOC through the q -axis stator current control to obtain maximum power at all wind speeds. T2FS is applied in AFSMOC to obtain adaptive gain the sliding mode control, so the robustness of controller can be improved. The advantages of VSMC are it can provide both sinusoidal line voltage and sinusoidal line current, so that the harmonics due switching frequency can be minimized. Simulation results shows that the AFSMOC can regulate the PMSG speed at optimum TSR so that the maximum power can be achieved at all wind speeds. VSMC also provide good performance for improve power quality of WTGs. Low harmonic for both line voltage and line current can be achieved with THD of line voltage with 0:35% and THD of line current 6.82%.

Acknowledgements

The first author would like to thank the Ministry of Research, Technology and Higher Education of Indonesia for their support through a doctoral research grant.

References

- [1] M. E. Haque, M. Negnevitsky, K. M. Muttaqi, "A Novel Control Strategy for a Variable-Speed Wind Turbine With a PMSG", *IEEE Trans. Industry Applications*, vol. 46, pp. 331–339, January 2010.
- [2] M. Chinchilla, S. Arnaltes, J. C. Burgos, "Control of Permanent-Magnet Generators Applied to Variable-Speed Wind-Energy Systems Connected to the Grid", *IEEE Trans. on Energy Conversion*, vol 21, pp. 130-135, March 2006.
- [3] Y. Chen, P. Pillay, A. Khan, "PM Wind Generator Topologies", *IEEE Trans. Industry Applications*, vol. 41, pp. 1619 – 1626, November 2005.
- [4] E. Mahersi, A. Khedher, M. F. Mimouni, "The Wind energy Conversion System Using PMSG Controlled by Vector Control and SMC Strategies", *International Journal of Renewable Energy Research*, Vol.3, pp. 42-50, 2013.
- [5] R. Melício, V.M.F. Mendes, J.P.S. Catalão, "Comparative study of power converter topologies and control strategies for the harmonic performance of variable-speed wind turbine generator systems", *Energy*, vol. 36, pp. 520–529, 2011.
- [6] A. Golshani, M. A. Bidgoli, S. M. T. Bathaee, "Design of Optimized Sliding Mode Control to Improve the Dynamic Behavior of PMSG Wind Turbine with NPC Back-to-Back Converter", *International Review of Electrical Engineering*, Vol. 8, pp. 1170-1180, 2013.
- [7] Y. Patel, A. Nasiri, "Multi-Level Wind Turbine Inverter to Provide Grid Ancillary Support", *International Journal of Renewable Energy Research*, Vol.4, pp. 999-1008, 2014.
- [8] A. Boukadoum, T. Bahi, D. Dib, "Fuzzy Logic Control Based Matrix Converter for Improvement Output Current Waveforms based Wind Turbine System", *International Journal of Renewable Energy Research*, Vol.3, pp. 587-591, 2013.
- [9] A. G. Yang, B. H. Li, "Application of A Matrix Converter for PMSG Wind Turbine Generation System", *2nd IEEE International Symposium on Power Electronics for Distributed Generation Systems*, China, pp. 185-189, 16-18 June 2010.
- [10] J. W. Kolar, T. Friedli, J. Rodriguez, and Patrick W, "Review of Three-Phase PWM AC–AC Converter Topologies", *IEEE Trans. Industrial Electronics*, vol. 58, pp. 4988–5006, November 2011.
- [11] J. W. Kolar, F. Schafmeister, S. D. Round, H. Ertl, Novel Three-Phase AC–AC Sparse Matrix Converters, *IEEE Trans. Power Electronics*, vol. 22, pp. 1649 – 1661, September 2007.
- [12] M. Aner, E. Nowicki, D. Wood, "Employing a Very Sparse Matrix Converter for Improved Dynamics of Grid-Connected Variable Speed Small Wind Turbines", *IEEE Power and Energy Conference at Illinois (PECI)*, Illionis, pp. 1-7, 24-25 February 2012.
- [13] F. F. M. El-Sousy, "Robust Wavelet Neural Network Sliding Mode Control System for Permanent Magnet Synchronous Motor Drive", *IET Elect Power Applications*, vol. 5, pp. 113 – 132, 2011.
- [14] C. Xia, X. Wang, S. Li, & X. Chen, "Improved integral sliding mode control methods for speed control of PMSM system", *Int. Journal of Innovative Computing, Information and Control*, vol. 7, pp. 1971-1982, 2011.
- [15] Q. Liang, J. M. Mendel, "Interval Type-2 Fuzzy Logic Systems: Theory and Design", *IEEE Trans. Fuzzy Systems*, vol. 8, pp. 535–550, October 2000.
- [16] J. M. Mendel, R. I. John, F. Liu, "Interval Type-2 Fuzzy Logic Systems Made Simple", *IEEE Trans. Fuzzy Systems*, vol. 14, pp. 808 – 821, December 2006.
- [17] Muldi Yuhendri, M. Ashari, M. H. Purnomo, "Maximum Output Power Tracking of Wind Turbine Using Intelligent Control", *TELKOMNIKA*, Vol.9, pp. 217-226, August 2011.

Appendix

PMSG data

Stator resistance	$R_s = 0.2 \Omega$
Stator inductance	$L_d = L_q = 8.5\text{mH}$
Pole pair numbers	$n_p = 4$
Flux of permanent magnet	$\psi_m = 0.175 \text{ Wb}$
Momen of inertia	$J = 0.089 \text{ kg m}^2$
Friction coefficient	$B = 0.005 \text{ N.m.s/rad}$

Wind Turbine Data

Blade radius	$R = 2 \text{ m}$
Maximum power coefficient	$C_{p_max} = 0.5312$
Optimum TSR	$\lambda_{opt} = 8.09$